



**Progress Report for the LIBRA Light Ion Beam Fusion  
Reactor Project for the Period January-June 1984**

**B. Badger, T.J. Bartel, M.L. Corradini, R.L. Engelstad, D.L.  
Henderson, G.L. Kulcinski, E.G. Lovell, G.A. Moses, K.J.  
O'Brien, R.R. Peterson, L. Pong, M.E. Sawan, I.N. Sviatoslavsky,  
W.F. Vogelsang, and J.J. Watrous**

**July 1984**

**FPA-84-1**

**FUSION POWER ASSOCIATES**

**2 Professional Drive, Suite 248  
Gaithersburg, Maryland 20879  
(301) 258-0545**

**1500 Engineering Drive  
Madison, Wisconsin 53706  
(608) 263-2308**

PROGRESS REPORT FOR THE LIBRA LIGHT ION BEAM FUSION REACTOR PROJECT  
FOR THE PERIOD JANUARY-JUNE 1984

B. Badger, T.J. Bartel, M.L. Corradini, R.L. Engelstad,  
D.L. Henderson, G.L. Kulcinski, E.G. Lovell, G.A. Moses,  
K.J. O'Brien, R.R. Peterson, L. Pong, M.E. Sawan,  
I.N. Sviatoslavsky, W.F. Vogelsang, J.J. Watrous

July 1984

FPA-84-1

## TABLE OF CONTENTS

|  | <u>PAGE</u> |
|--|-------------|
| 1. Introduction                        | 1-1         |
| 2. Channel MHD Computer Code           | 2-1         |
| 3. Ion Beam Propagation                | 3-1         |
| 4. Mechanical Analysis of INPORT Units | 4-1         |
| 5. Target Chamber Gas Dynamics         | 5-1         |

## 1. Introduction

This is a progress report of work performed between January 1, 1984 and June 30, 1984 by Fusion Power Associates under contract to Kernforschungs-zentrum Karlsruhe. The purpose of the work is to analyze some key issues associated with the design of the LIBRA light ion beam fusion reactor. This work includes:

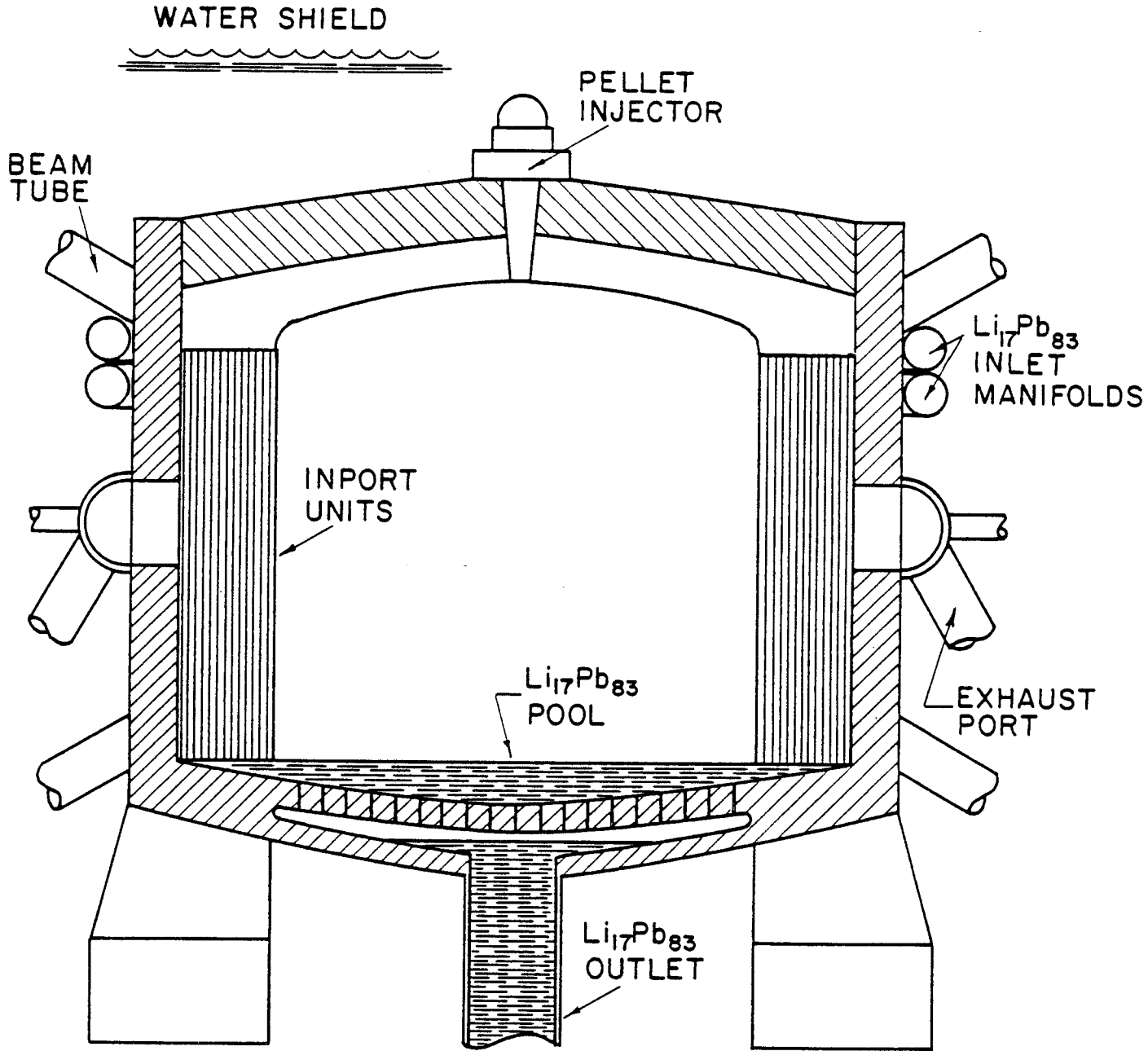
1. development of a plasma MHD computer code for preformed plasma channel design;
2. development of ion propagation codes to predict ion propagation in plasma channels;
3. further analysis of INPORT tube response; and
4. target chamber gas dynamics.

Parameters for the LIBRA design are given in Table 1.1 with a cross-sectional view shown in Fig. 1.1. The critical issues for LIBRA are associated with the propagation of ions from the diodes to the target and with the gas filled cavity response following the microexplosion.

Papers related to LIBRA that have been published or will soon be published are:

1. K.J. O'Brien, "Adiabatic Particle Beam Model: Resonant Modification of Adiabatic Invariant," to be presented at APS Plasma Physics Meeting, Boston, MA, November 1984.
2. R.R. Peterson, J.J. Watrous and G.A. Moses, "Microfireball Propagation in Z-Pinch Plasma Channels," to be presented at APS Plasma Physics Meeting, Boston, MA, November 1984.
3. R.L. Engelstad and E.G. Lovell, "Mechanical Response and Stability of INPORT Tubes for ICF Reactors," 13th Symposium on Fusion Technology, Varese, Italy, September 1984.
4. R.L. Engelstad and E.G. Lovell, "Analysis of Modal Coupling of Coolant Tubes for Inertial Fusion Applications," 3rd International Modal Analysis Conference, Orlando, FL, January 1985.
5. R.L. Engelstad, "Planar Vibrations of LIBRA INPORT Tubes Including Gravity Gradient Effects," Fusion Power Associates Report FPA-84-2, July 1984.
6. R.L. Engelstad, "Basic Theory for Three-Dimensional Motion of LIBRA INPORT Tubes," Fusion Power Associates Report FPA-84-3, July 1984.

Fig. 1.1



SCHEMATIC OF LIBRA REACTION CHAMBER

Table 1.1. Major LIBRA Parameters

|                       |  |
|-----------------------|--|
| Reactor Type          | Demonstration, Electricity Production  |
| Cost Goal             | Less than $10^9$ \$                    |
| Ion Accelerator Type  | Pulsed Power Diode or Multi-Stage      |
| First Wall Protection | HIBALL-like INPORT Units               |
| Ion Propagation Mode  | Preformed Channels or Self-Propagation |
| Target Yield          | 320 MJ                                 |
| Repetition Rate       | 1.5 Hz                                 |
| Fusion Power          | 480 MW                                 |
| Thermal Power         | 612 MW                                 |
| Gross Electric Power  | 245 MW                                 |
| Net Electric Power    | 215 MW                                 |

## 2. Channel MHD Computer Code

A computer code called Z-PINCH has been developed to describe the creation of plasma channels and the response of channels to the passage of an ion beam. The theory used in this code has been reported in earlier progress reports and will not be repeated here. The Z-PINCH code<sup>(1)</sup> is a combination of radiation-hydrodynamics from MF-FIRE,<sup>(2)</sup> equations of state and opacities from MIXERG,<sup>(3)</sup> magnetic field diffusion and convection from MAGPIE,<sup>(4)</sup> and external circuit modeling from WHYRAC.<sup>(5)</sup> The fundamentals of the Z-PINCH code have been completed and tested. The Z-PINCH code has been used to verify the results of Freeman, Baker and Cook<sup>(6)</sup> and shows good agreement with their calculations. The first version of the Z-PINCH code has been delivered to KfK and will be implemented on their computer system. Further testing and enhancement of the code is expected as more experience is gained in using it. The last few progress reports have followed the development of this code from the initial proposal, through the testing of individual modules. In this report we present full scale results of the code.

The problem to be simulated consists of a laser initiated low temperature argon plasma at a density of  $2.25 \times 10^{-5}$  g/cm<sup>3</sup> through which a two-stage current pulse is discharged. The current pulse shape is shown in Fig. 2.1. This two-stage current pulse is modeled as a succession of two critically damped LRC circuits, Fig. 2.2. Figures 2.3-2.11 show various quantities output by the Z-PINCH code. Each of these figures is compared with the results of Freeman, Baker and Cook where possible. The R-T plots, Fig. 2.3, show the trajectories of the Lagrangian zones and are an excellent way of visualizing the channel dynamics. The first current pulse is small enough that the expansive force due to Joule heating dominates over the  $\underline{J} \times \underline{B}$  pinching force of the magnetic field. A shock wave is driven outward, evacuating the channel to less than 10% of its initial density. The second, stronger pulse, creates a strong magnetic field which pinches the channel very rapidly. The ion beam is injected into the channel shortly after 5  $\mu$ s, once the magnetic field is established but before the field has time to pinch the channel. The other figures show the radial profiles of the hydrodynamic quantities during the first and second current pulses. Figure 2.11 shows a roughly linear magnetic field with a maximum of nearly 20 kG at 5.3  $\mu$ s.

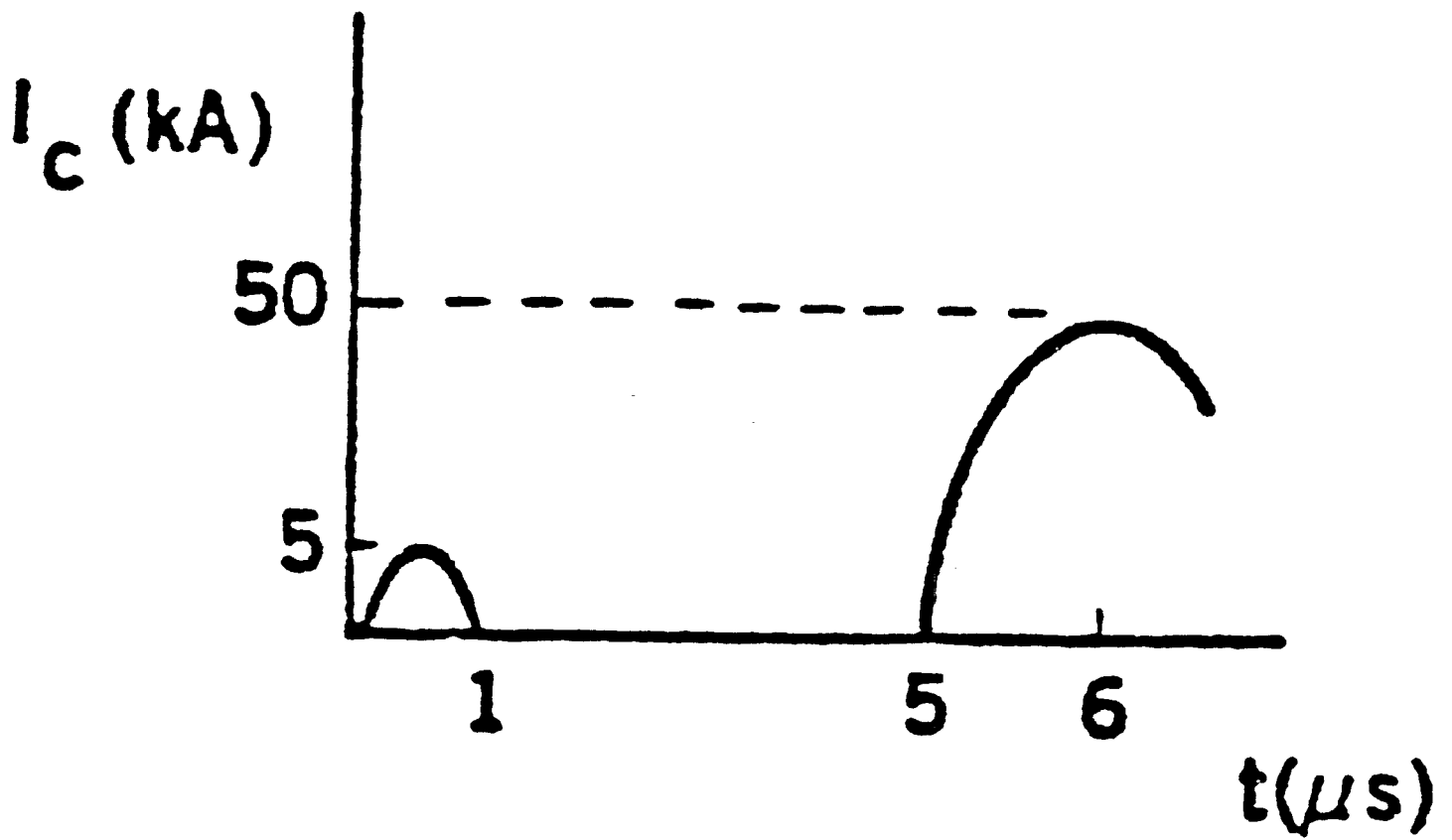


Fig. 2.1. Two-stage current pulse.



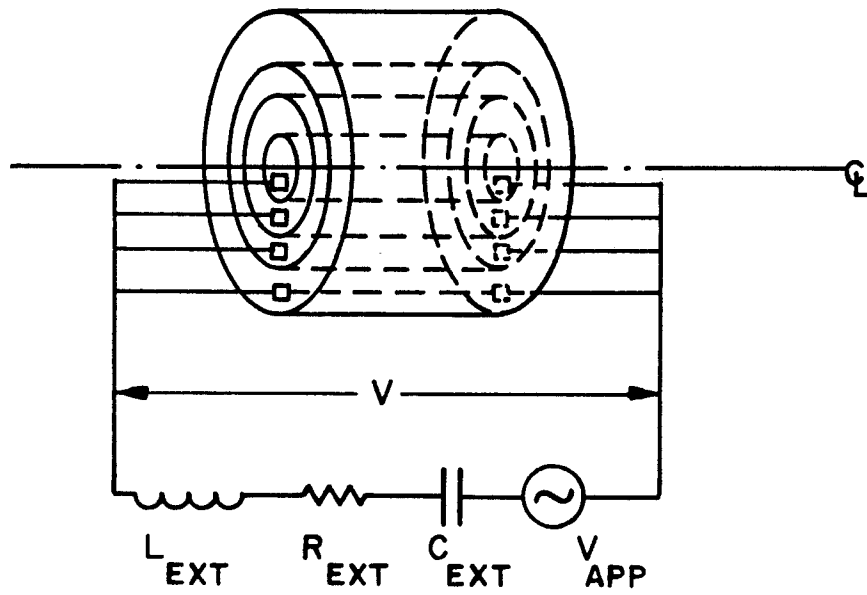


Fig. 2.2. External circuit.

# R-T PLOT FOR ZONES

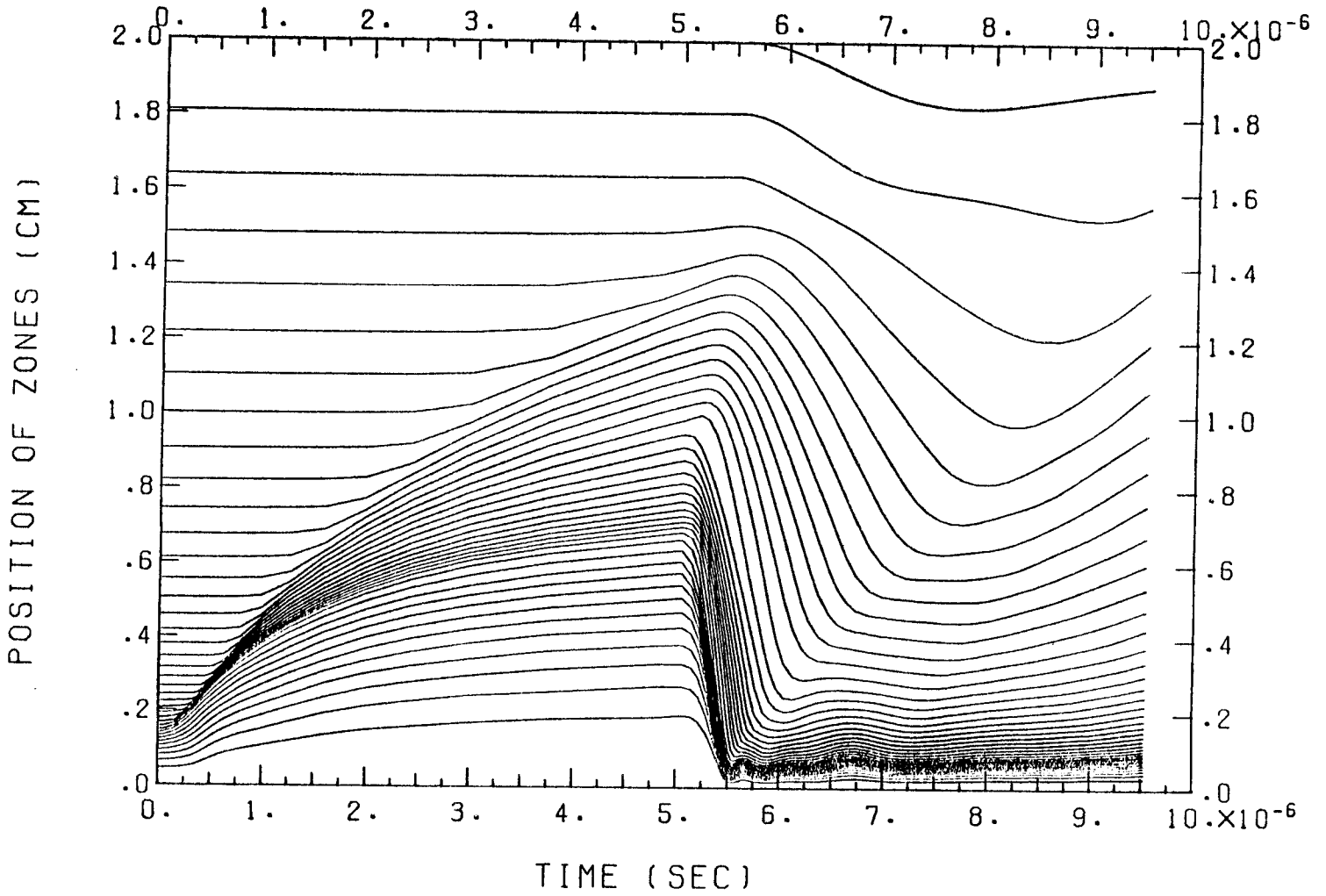


Fig. 2.3. R-T plot for zones.

# PLASMA TEMPERATURE

- 1 T = .2572-03 MSEC
- 2 T = .4615-03 MSEC
- 3 T = .5380-03 MSEC
- 4 T = .1000-02 MSEC
- 5 T = .3009-02 MSEC
- 6 T = .3765-02 MSEC

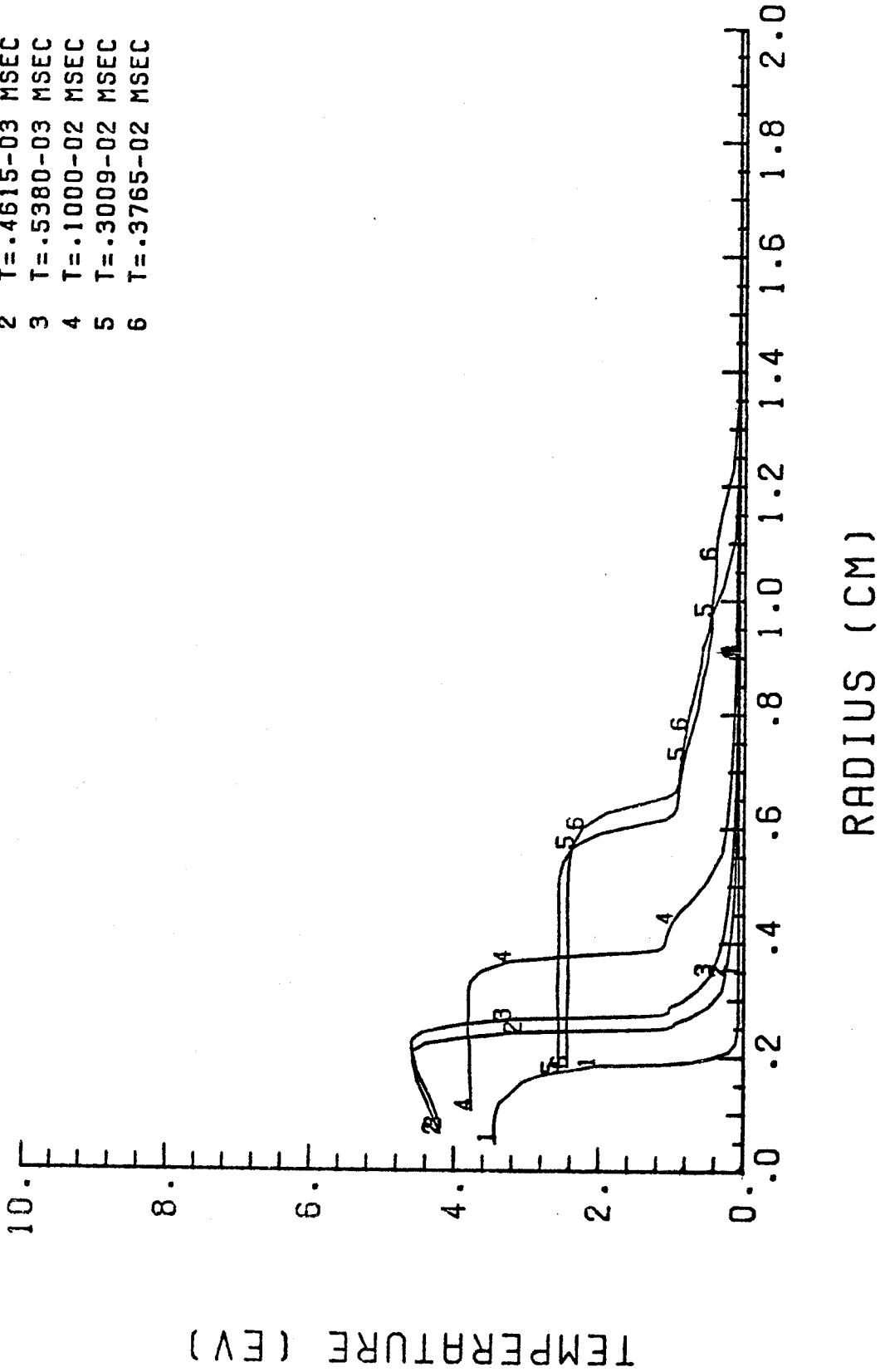


Fig. 2.4. Plasma temperature during first current pulse.

# PLASMA DENSITY

- 1 T=.2572-03 MSEC
- 2 T=.4615-03 MSEC
- 3 T=.5380-03 MSEC
- 4 T=.1000-02 MSEC
- 5 T=.3009-02 MSEC
- 6 T=.3765-02 MSEC

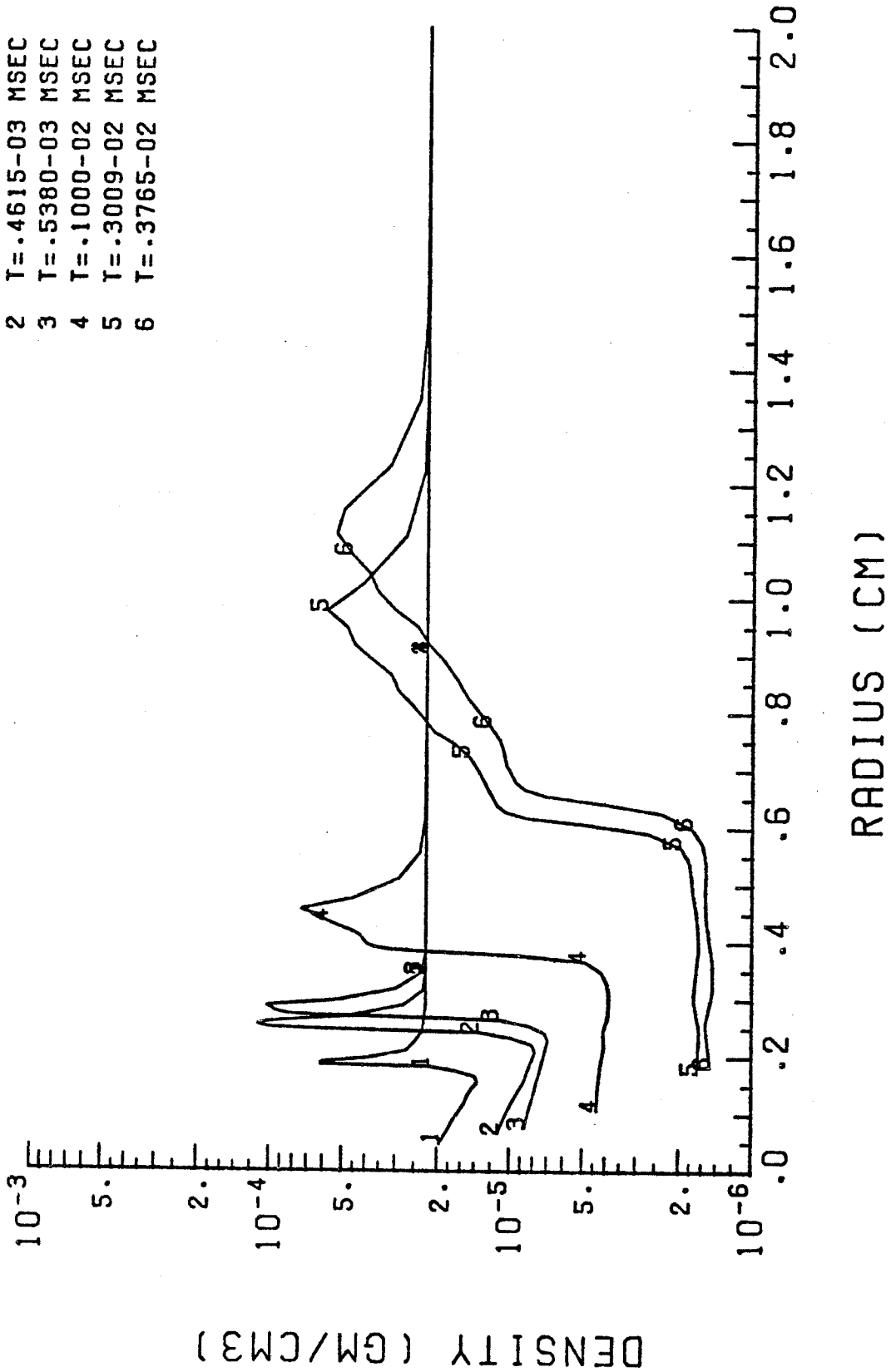


Fig. 2.5. Plasma density during first current pulse.

# FLUID VELOCITY

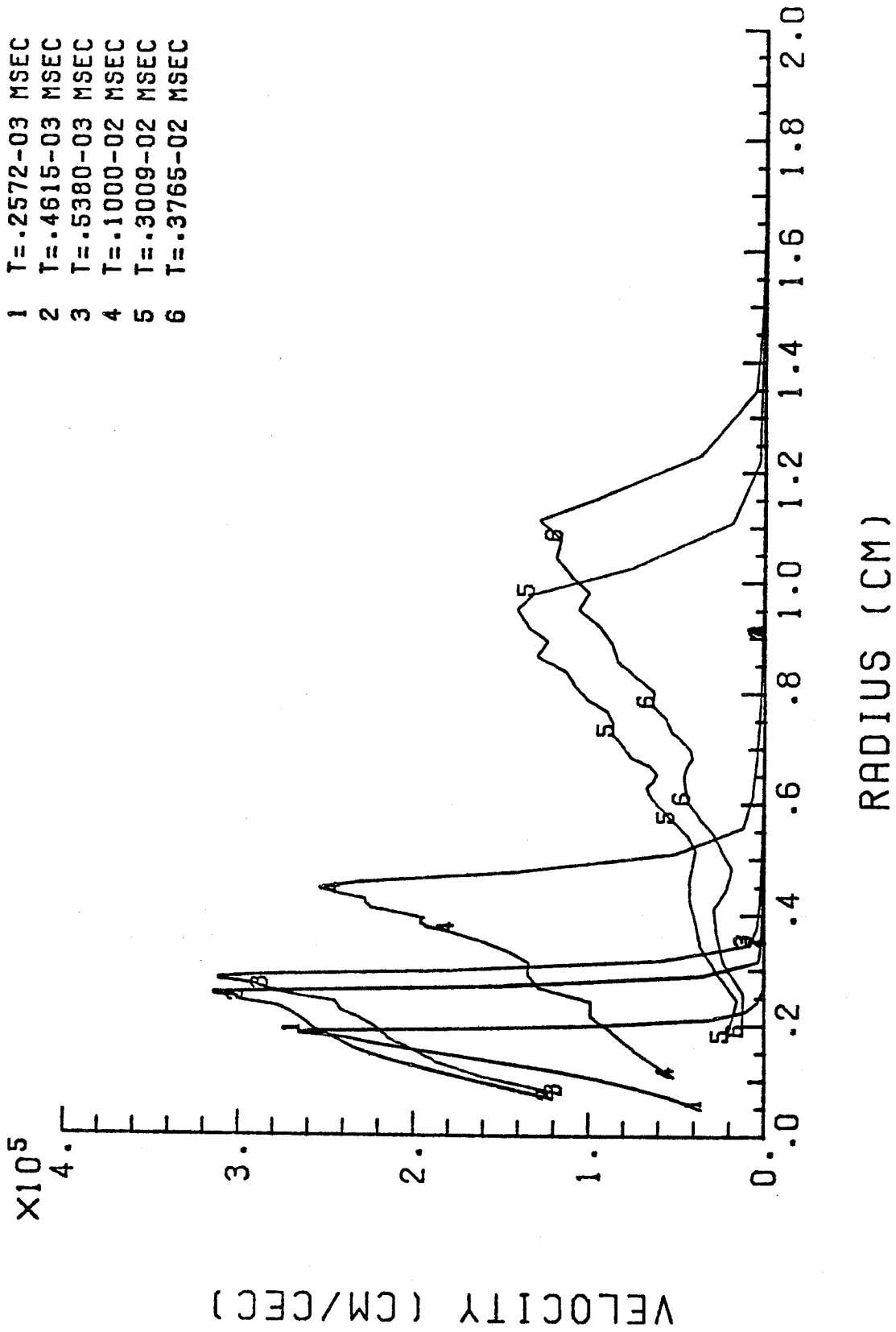


Fig. 2.6. Fluid velocity during first current pulse.

# MAGNETIC FIELD

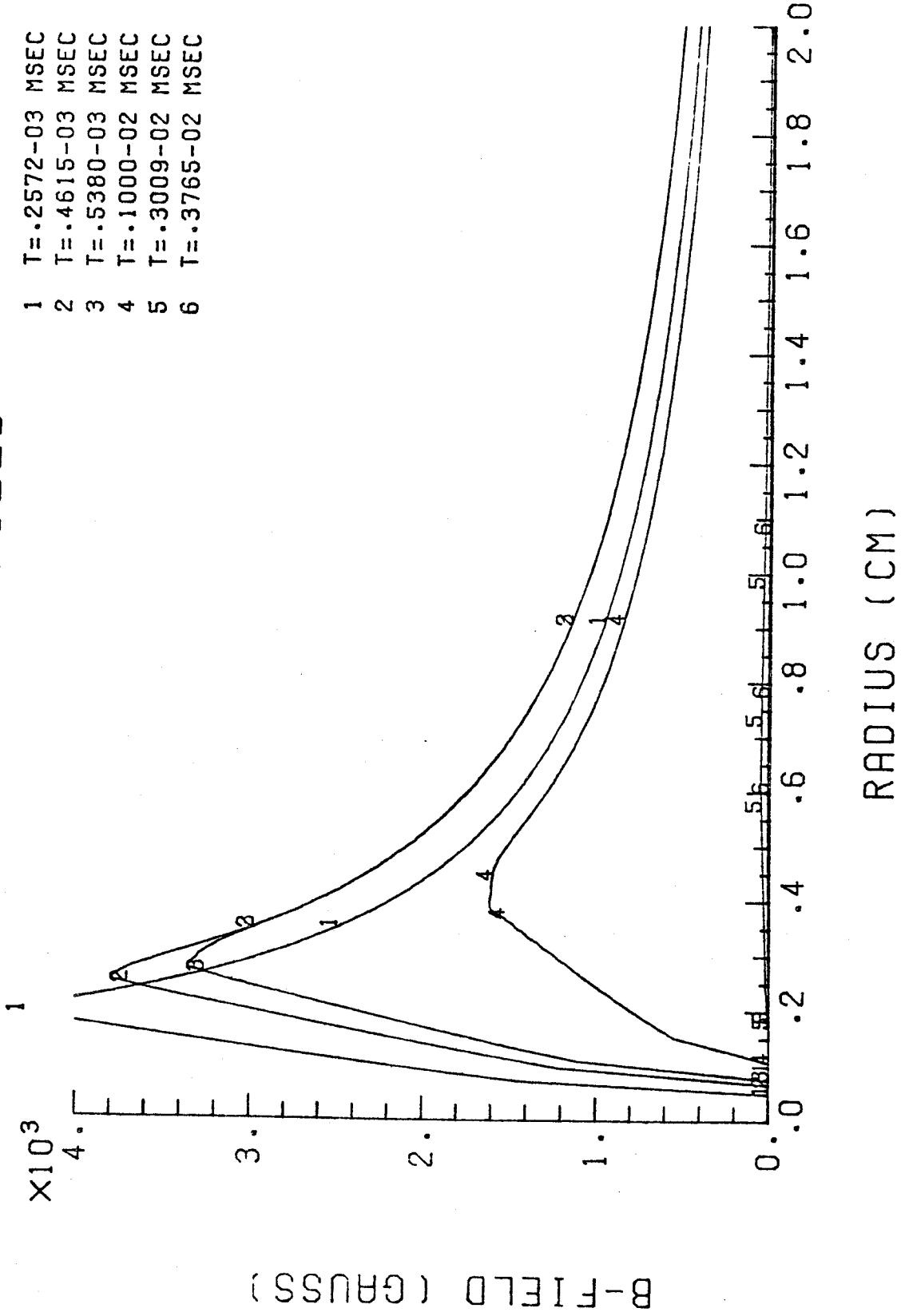


Fig. 2.7. Magnetic field during first current pulse.

# PLASMA TEMPERATURE

- 1 T=.4808-02 MSEC
- 2 T=.5058-02 MSEC
- 3 T=.5302-02 MSEC
- 4 T=.5521-02 MSEC

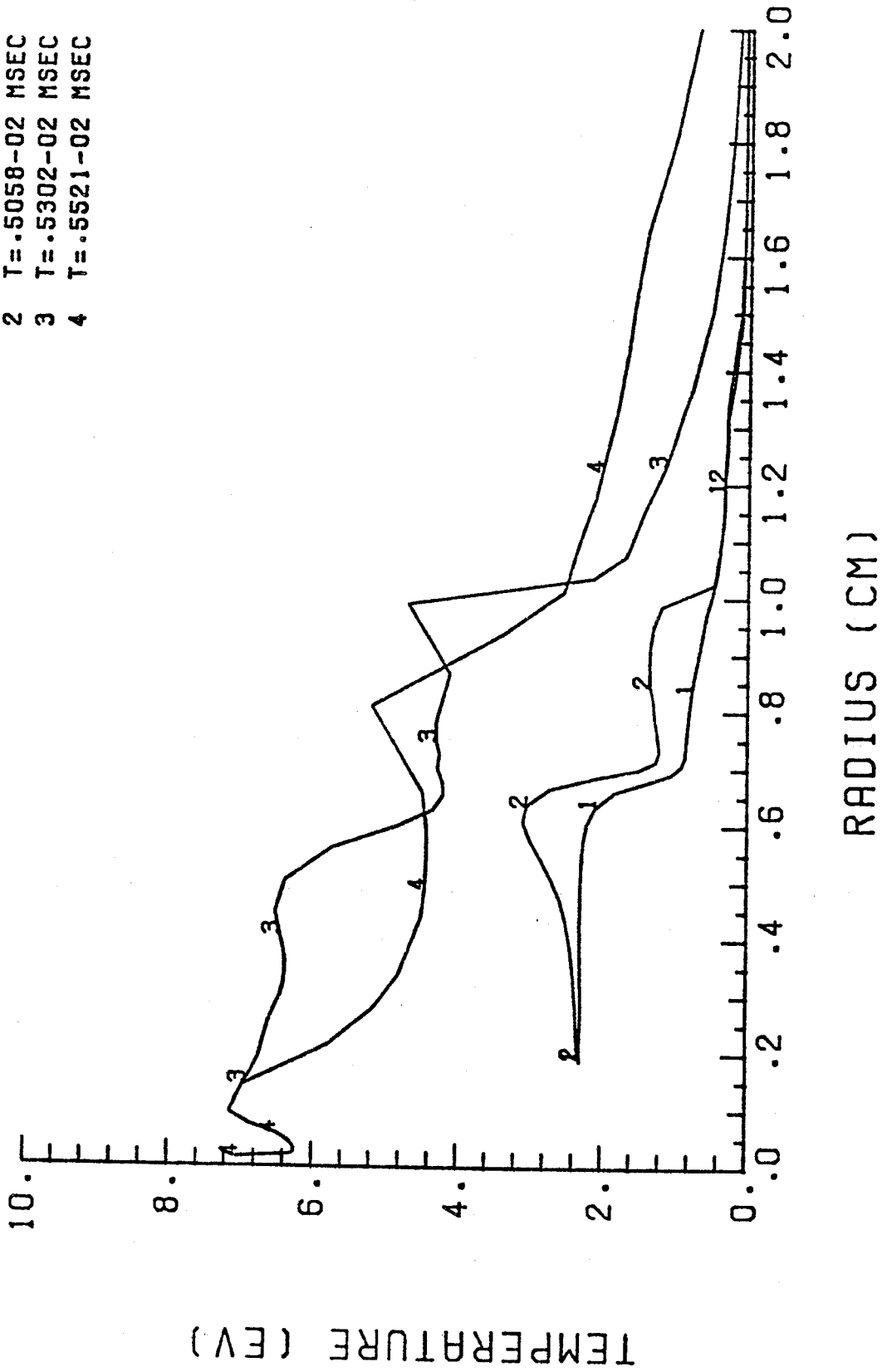


Fig. 2.8. Plasma temperature during second current pulse.

# PLASMA DENSITY

- 1 T=.4808-02 MSEC
- 2 T=.5058-02 MSEC
- 3 T=.5223-02 MSEC
- 4 T=.5521-02 MSEC

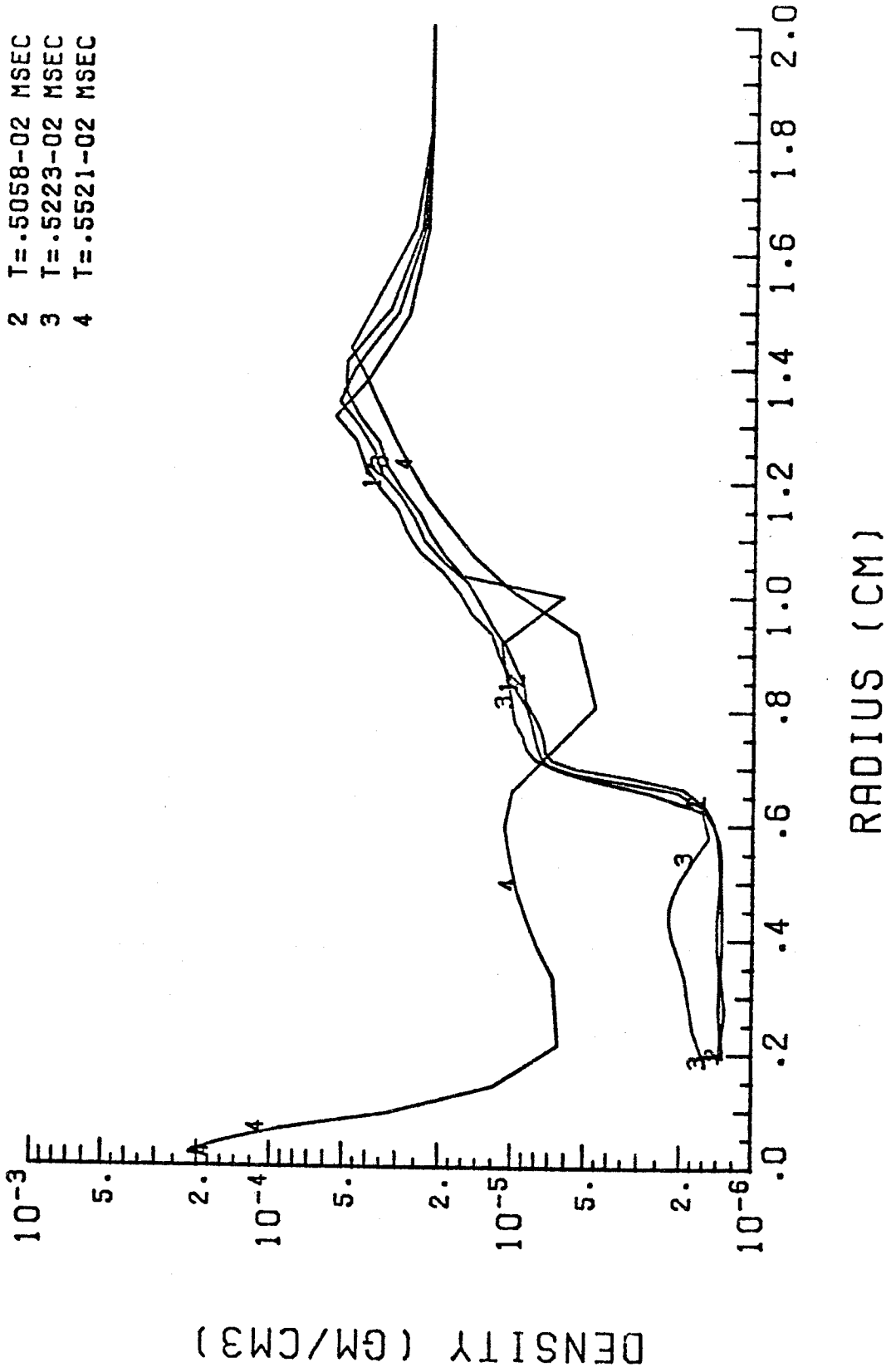


Fig. 2.9. Plasma density during second current pulse.



# FLUID VELOCITY

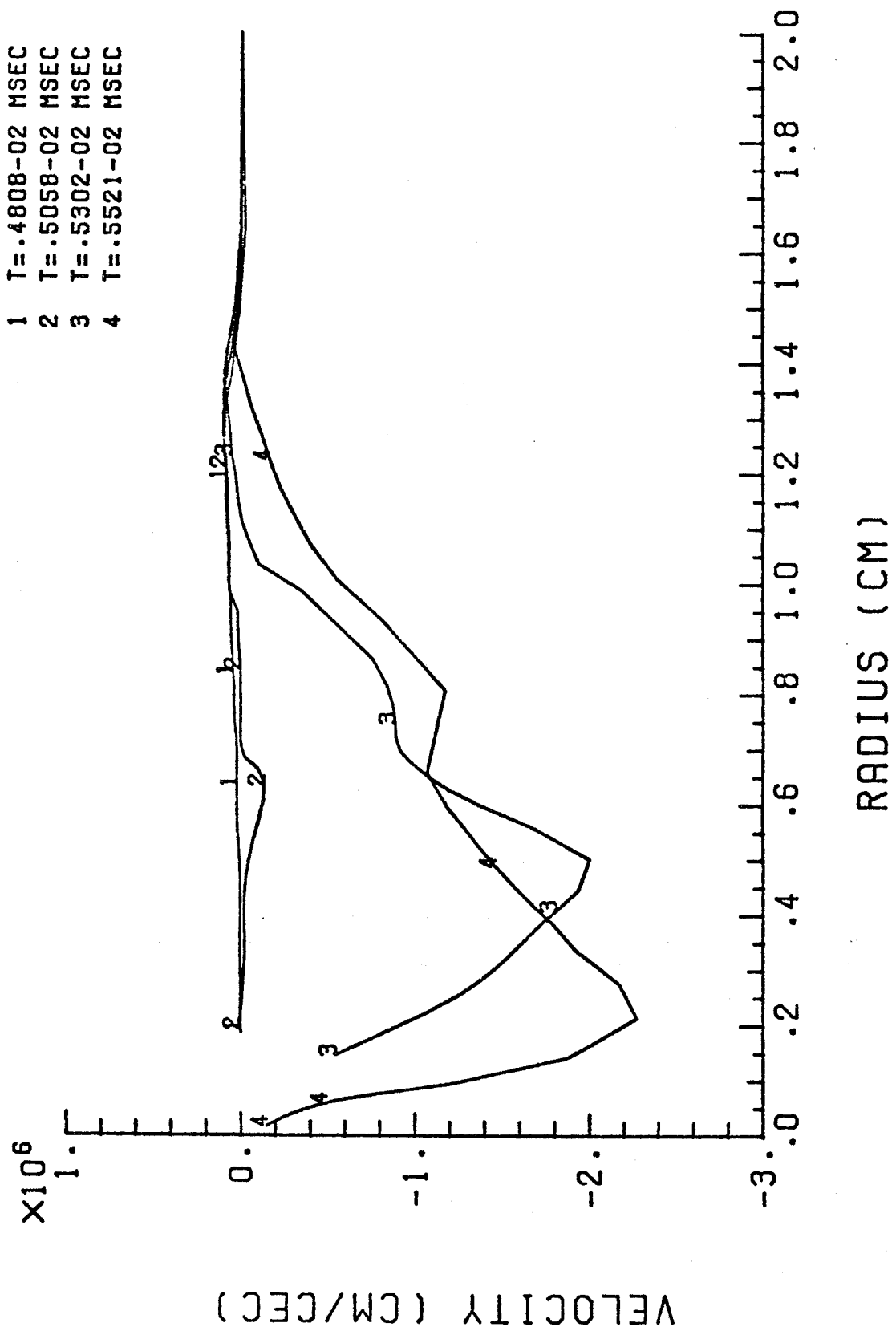


Fig. 2.10. Fluid velocity during second current pulse.

# MAGNETIC FIELD

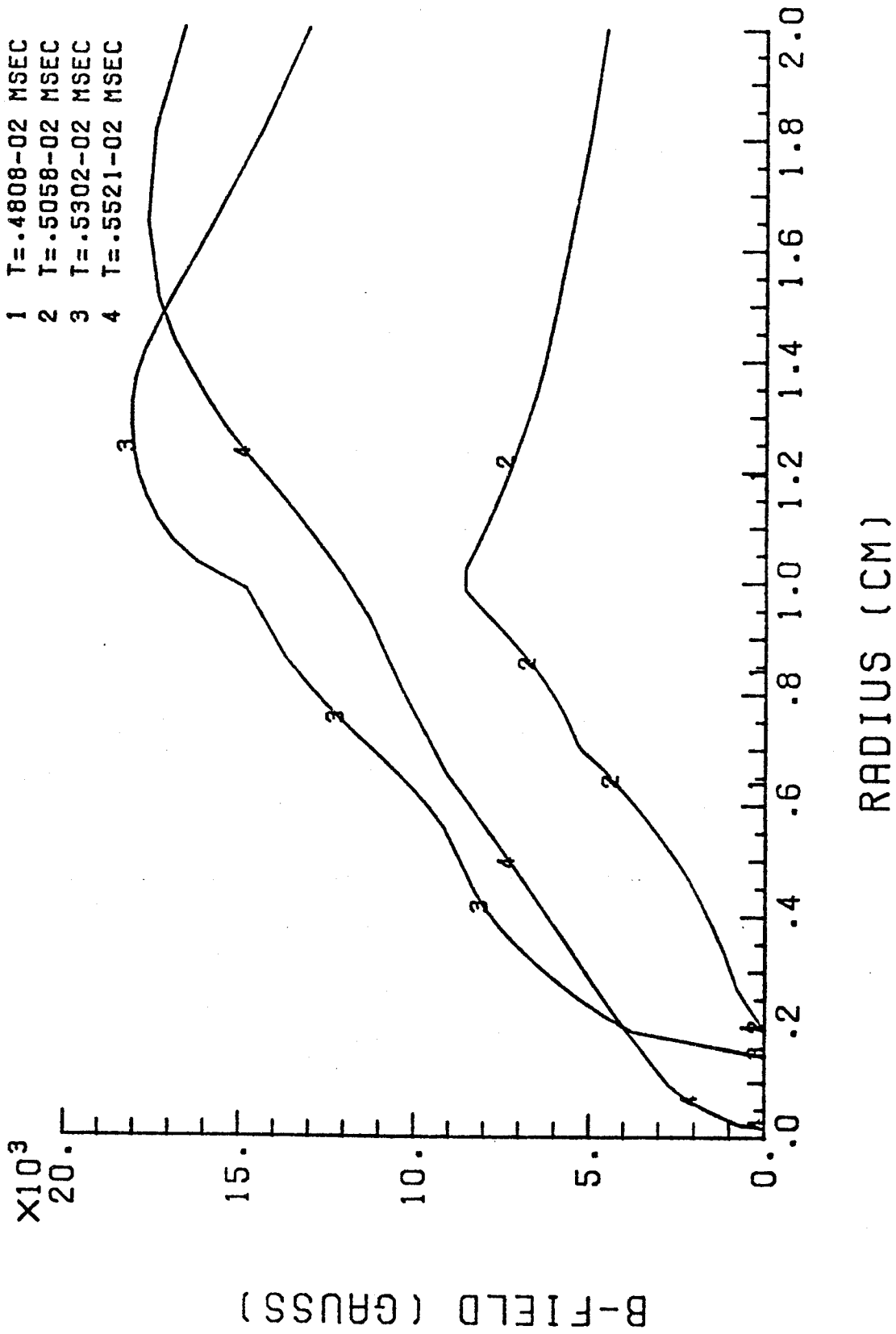


Fig. 2.11. Magnetic field during second current pulse.

Channel design calculations for LIBRA have not yet been done. This will follow in the second half of this contract period.

#### References for Section 2

1. J.J. Watrous, G.A. Moses and R.R. Peterson, "Z-PINCH - A Magnetohydrodynamic Radiative Transfer Computer Code," University of Wisconsin Fusion Engineering Program Report UWFDM-584, June 1984.
2. G.A. Moses, T.J. McCarville and R.R. Peterson, "MF-FIRE - A Multifrequency Radiative Transfer Hydrodynamics Code," University of Wisconsin Fusion Engineering Program Report UWFDM-458, December 1982.
3. R.R. Peterson and G.A. Moses, "MIXERG - An Equation of State and Opacity Computer Code," Comp. Phys. Comm. 28, 405 (1983).
4. D. Steinberg, R. Kider and A. Cecil, "A One-Dimensional Magnetohydrodynamics Code," Lawrence Livermore National Laboratory Report UCRL-14931, June 1966.
5. D.G. Colombant and M. Lampe, "WHYRAC - A New Modular One-Dimensional Exploding Wire Code," Naval Research Laboratory Memorandum Report 3726, February 1978.
6. J. Freeman, L. Baker and D. Cook, "Plasma Channels for Intense-Light-Ion-Beam Reactors," Nucl. Fusion 22, 383 (1982).

### 3. Ion Beam Propagation

During this first half of the current contract period we have accumulated a great amount of information regarding the propagation of ion beams in general. This information has been reviewed in detail and a copy of this review material has been delivered to KfK. We are not at the same stage of development in ion propagation simulation as we are in plasma MHD simulation. We have written two easy-to-use codes that embody the work of Ottinger, Mosher and Goldstein.<sup>(1-3)</sup>

One of these codes, ION, computes the trajectories of individual ions undergoing betatron oscillations in a perfectly space and current neutralizing channel.<sup>(1)</sup> This code allows us to gain an intuitive understanding of ion propagation in both uniform and tapered z-pinch channels. Since we have previously reported results for straight currents we choose to use the tapered channel as our example in this progress report. Table 3.1 specifies the parameters used for the calculation and Figs. 3.1-3.5 show the results of the calculations. Figure 3.1 shows a snapshot in time of the ion positions in a tapered channel with a 20 cm taper length. We see that, just as stated by Ottinger, Mosher and Goldstein, the ion trajectories do not converge as fast as the channel radius, hence ions are lost. Figures 3.2-3.5 show radial profiles of the number of ions and ion intensity measured at the beginning and end of the taper length. These figures clearly show the focusing of the beam by the increasing magnetic field. Such calculations will allow us to evaluate the active focusing at the target suggested by Goldstein.

The other code, WINDOW, predicts the allowable ion current in a channel as a function of the divergence angle of the beam for constraints imposed by five instability conditions: (1) electrostatic (ES), (2) beam filamentation (BFIL), (3) channel filamentation (CFIL), (4) MHD expansion (MHD), and (5) beam energy loss (ELOSS).<sup>(2-3)</sup> The WINDOW code has been used to analyze beam conditions proposed by Ian Smith in his design of the pulsed power driver.<sup>(4)</sup> These WINDOW calculations are summarized in Table 3.2 and displayed in Figs. 3.6-3.11. In these figures, stable regions in the plane of beam power per channel versus ion beam divergence are plotted for a variety of ion species, ion energies and beam pulse widths. In all cases, the channel radius is 0.5 cm and the gas density is the optimum. These windows of stability are bounded by limits imposed by the five criteria mentioned earlier.

Table 3.1. Tapered Channel Parameters

30 MeV  $\text{Li}^{+3}$   
 17 ns pulse  
 20 cm channel taper length  
 2 cm channel radius  
 1 cm focal spot radius  
 0.075 radian maximum injection angle  
 27.48 kA channel current

Table 3.2. Propagation of Ions in Plasma Channels

| Case #                                       | 1               | 2               | 3                | 4                | 5                | 6                |
|--|-----------------|-----------------|------------------|------------------|------------------|------------------|
| Ion species                                  | $\text{D}^{+1}$ | $\text{D}^{+1}$ | $\text{Li}^{+3}$ | $\text{Li}^{+3}$ | $\text{Li}^{+3}$ | $\text{Li}^{+3}$ |
| Particle energy (MeV)                        | 15              | 15              | 30               | 30               | 64               | 64               |
| Pulse width at diode (ns)                    | 50              | 17              | 50               | 17               | 50               | 17               |
| Pulse width at target (ns)                   | 17              | 17              | 17               | 17               | 17               | 17               |
| Optimum beam divergence<br>(radians)         | 0.11            | 0.135           | 0.09             | 0.13             | 0.09             | 0.125            |
| Maximum power per channel at<br>diode (TW)   | 15              | 125             | 3                | 20               | 18               | 140              |
| Proposed power per channel at<br>diode (TW)  | 5               | 14              | 6                | 19               | 19.2             | 32               |
| Proposed power per channel at<br>target (TW) | 10              | 10              | 13.5             | 13.5             | 41.6             | 24               |
| Proposed # of channels                       | 27              | 27              | 18               | 18               | 6                | 10               |

# ION POSITIONS

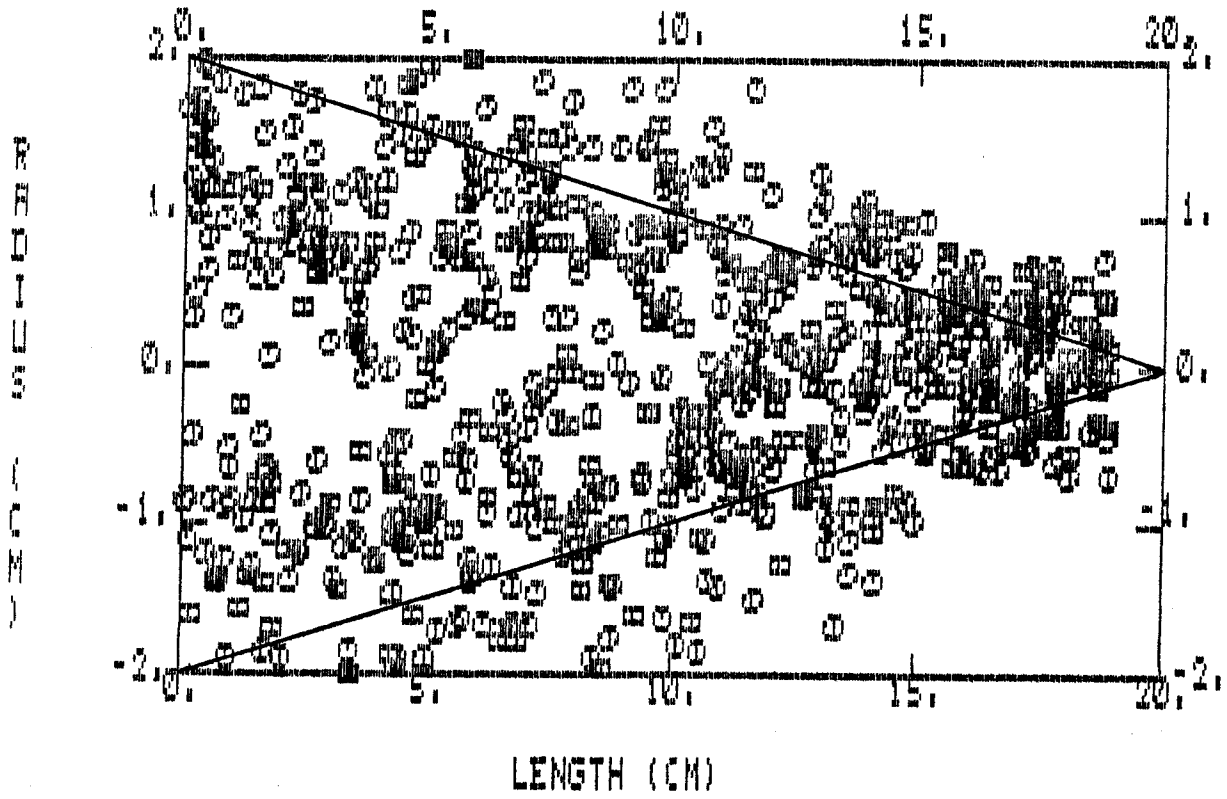


Fig. 3.1. Ion positions in tapered channel.

### RADIAL ION DISTRIBUTION

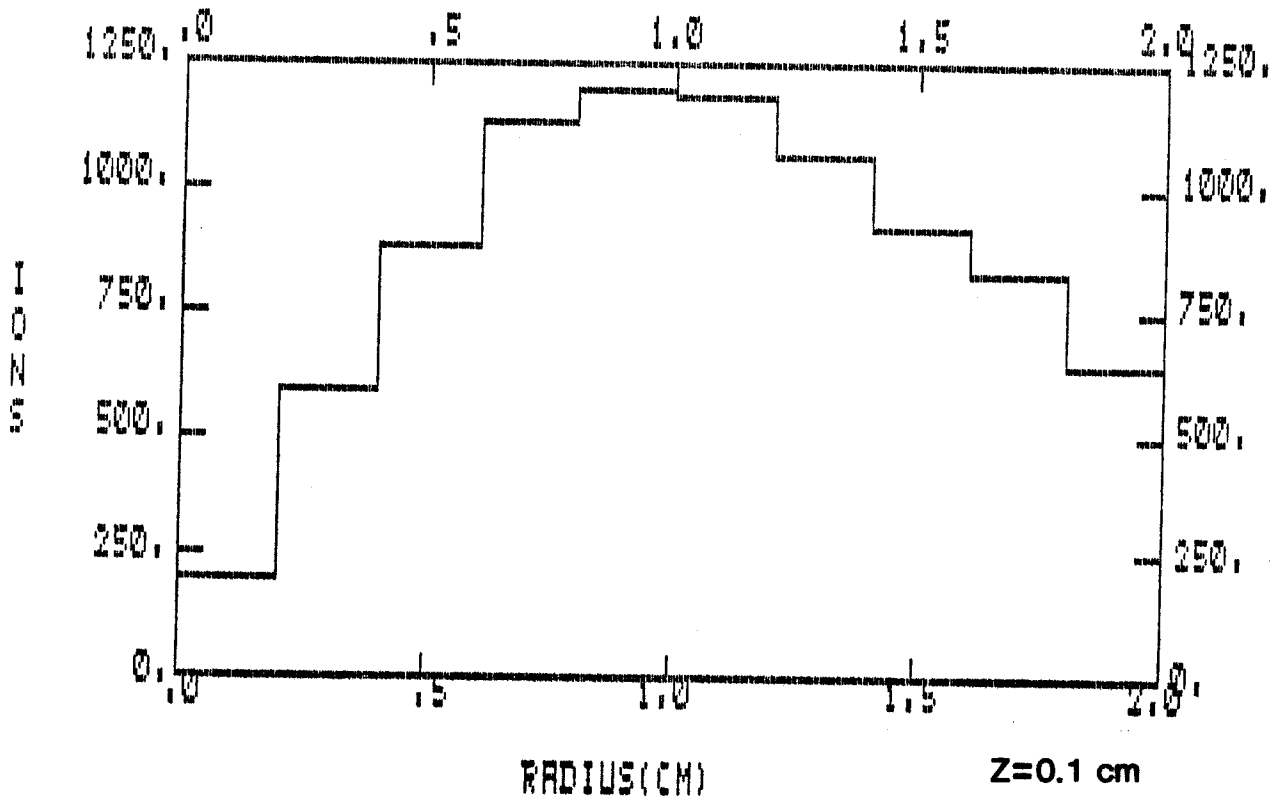


Fig. 3.2. Radial ion distribution at beginning of tapered channel.

### RADIAL ION DISTRIBUTION

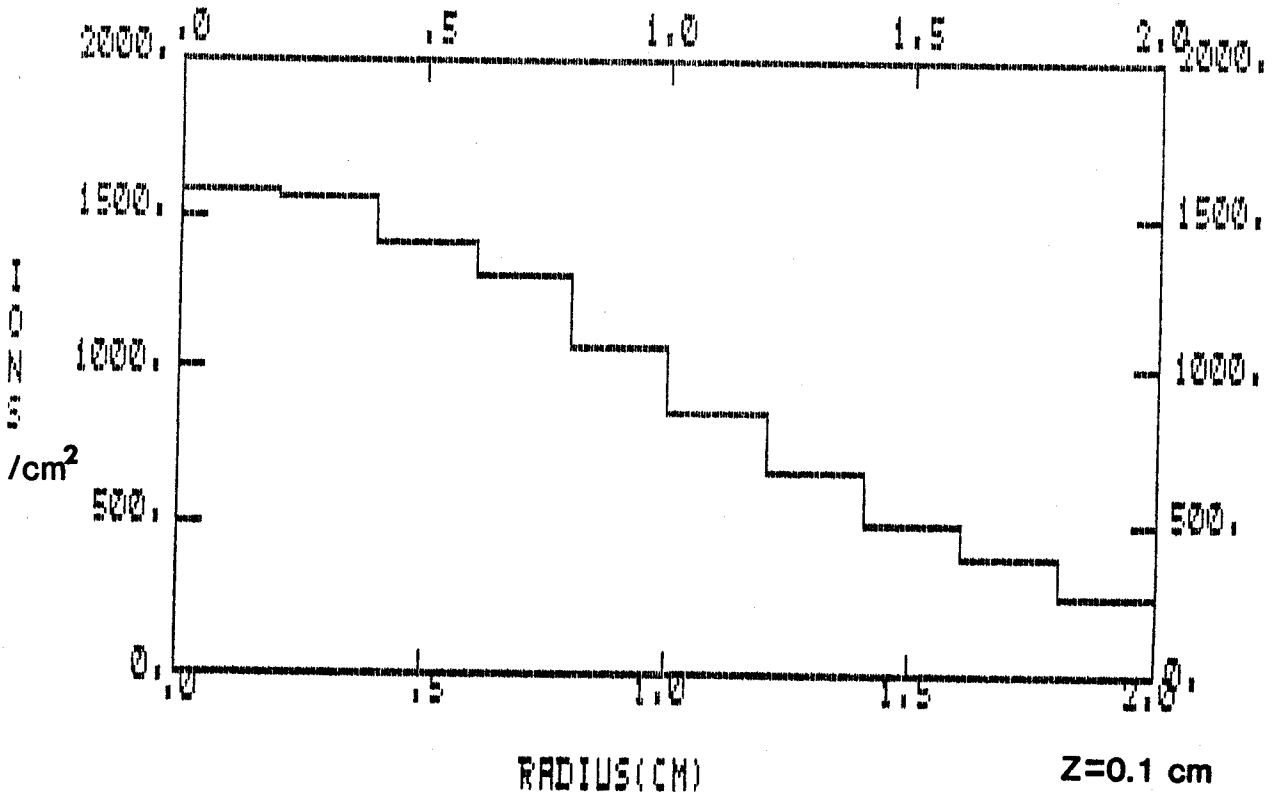


Fig. 3.3. Radial ion density at beginning of tapered channel.



### RADIAL ION DISTRIBUTION

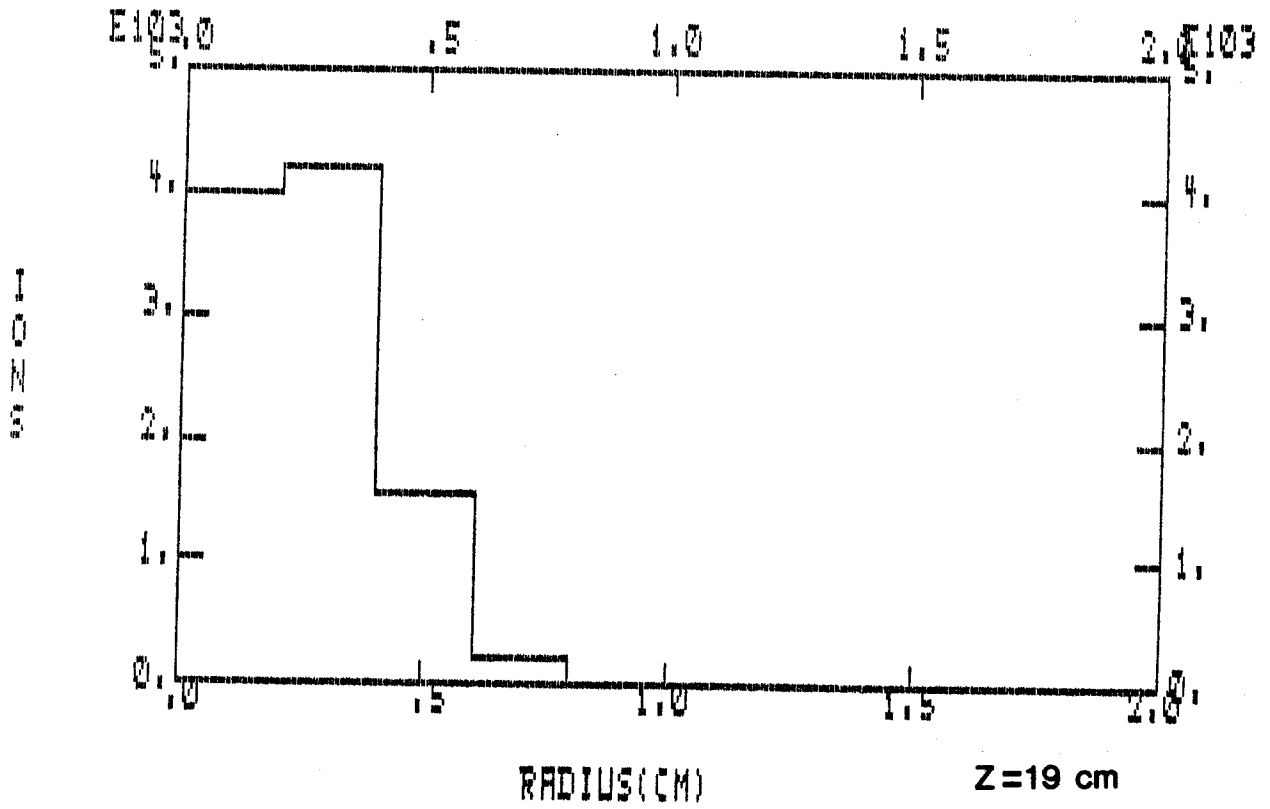


Fig. 3.4. Radial ion distribution at end of tapered channel.

### RADIAL ION DISTRIBUTION

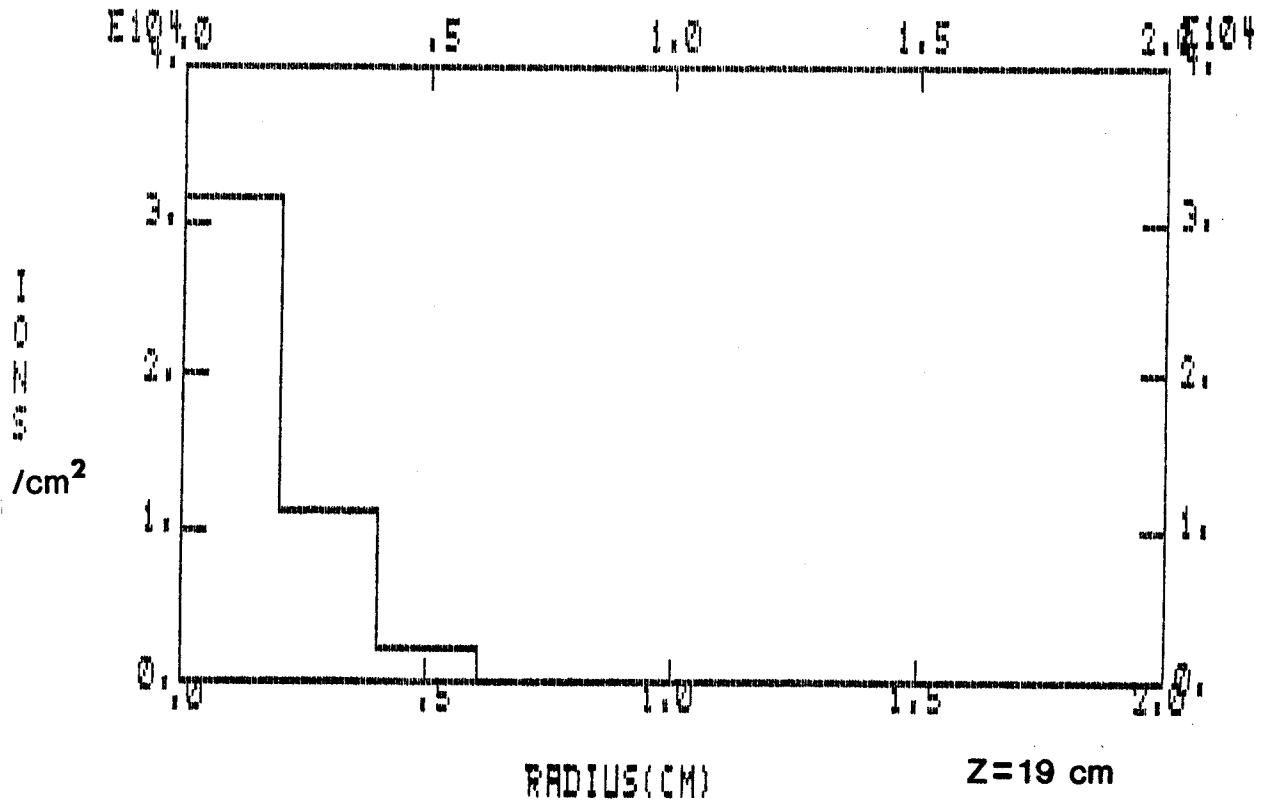
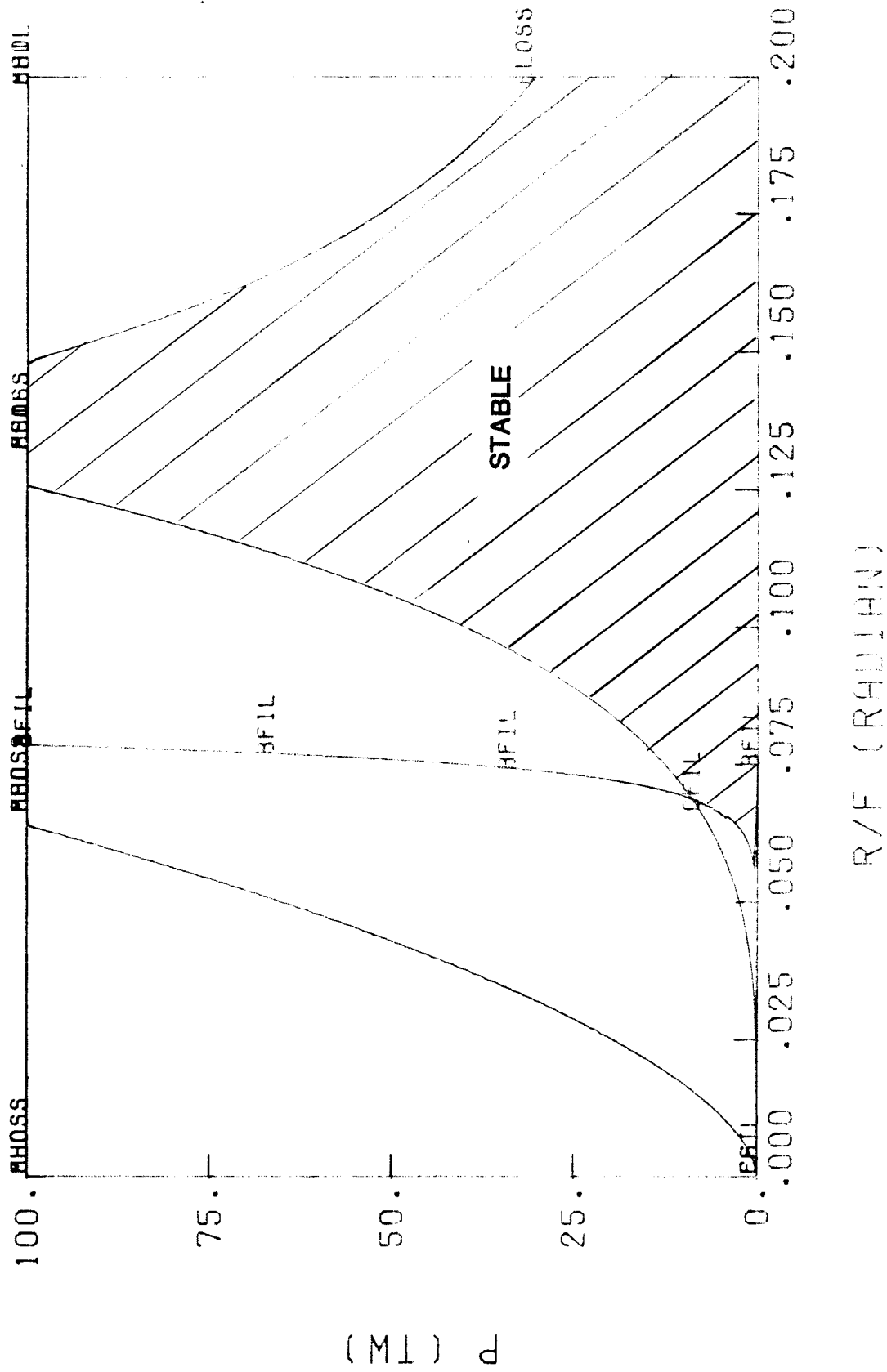


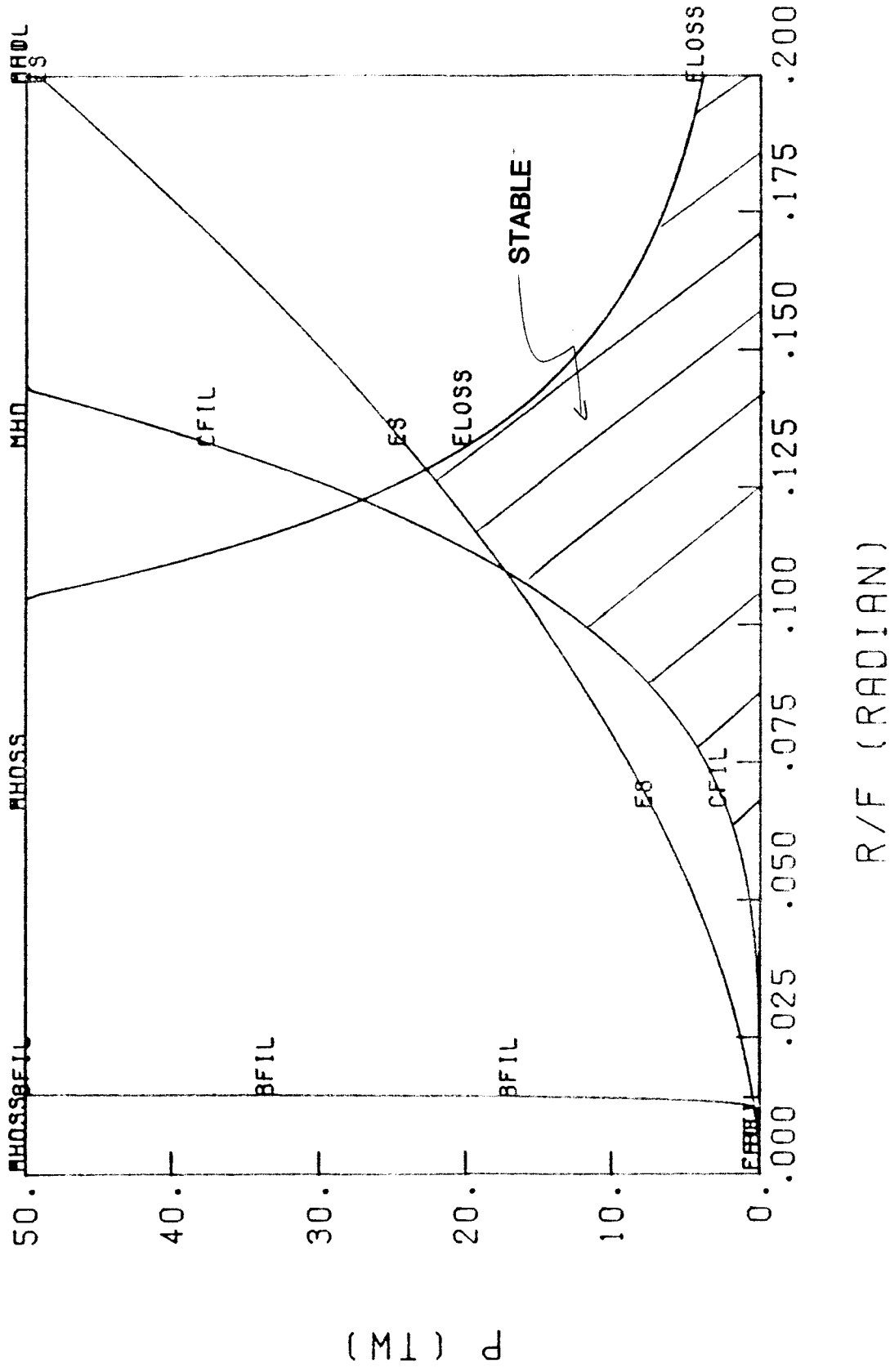
Fig. 3.5. Radial ion density at end of tapered channel.



ABEAM= 2.0 AMU ZBEAM=1.0 E RBEAM= .5 CM TBEAM=.1700-07 S X=1.0 EBAR=15.0 MEV

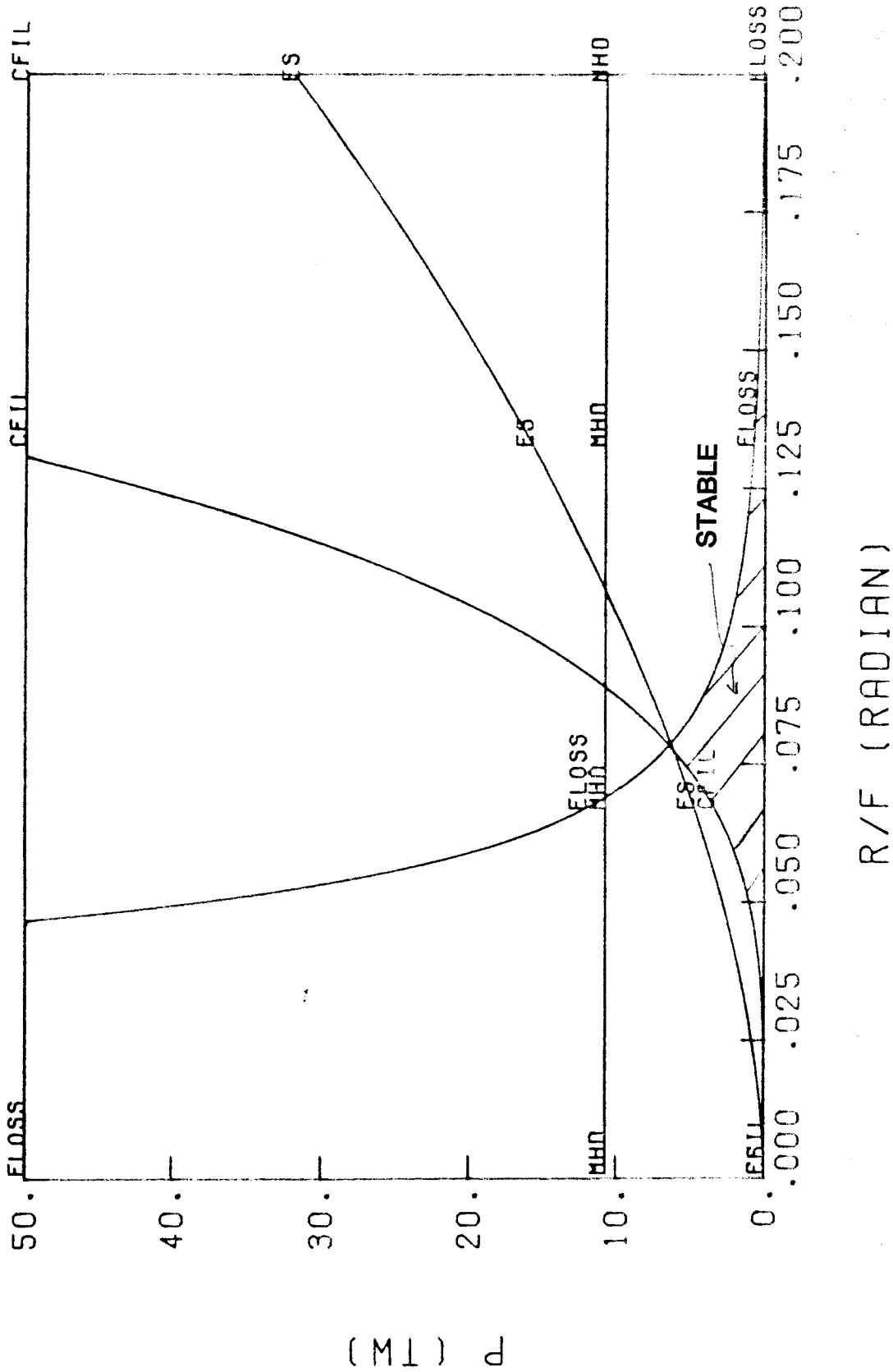
Fig. 3.6. Stability regions in power vs. beam divergence space for a pulse of 15 MeV D 17 ns long.





ABEAM= 7.0 AMU ZBEAM=3.0 E RBEAM= .5 CM TBEAM=.1700-07 S X=1.0 EBAR=30.0 MEV

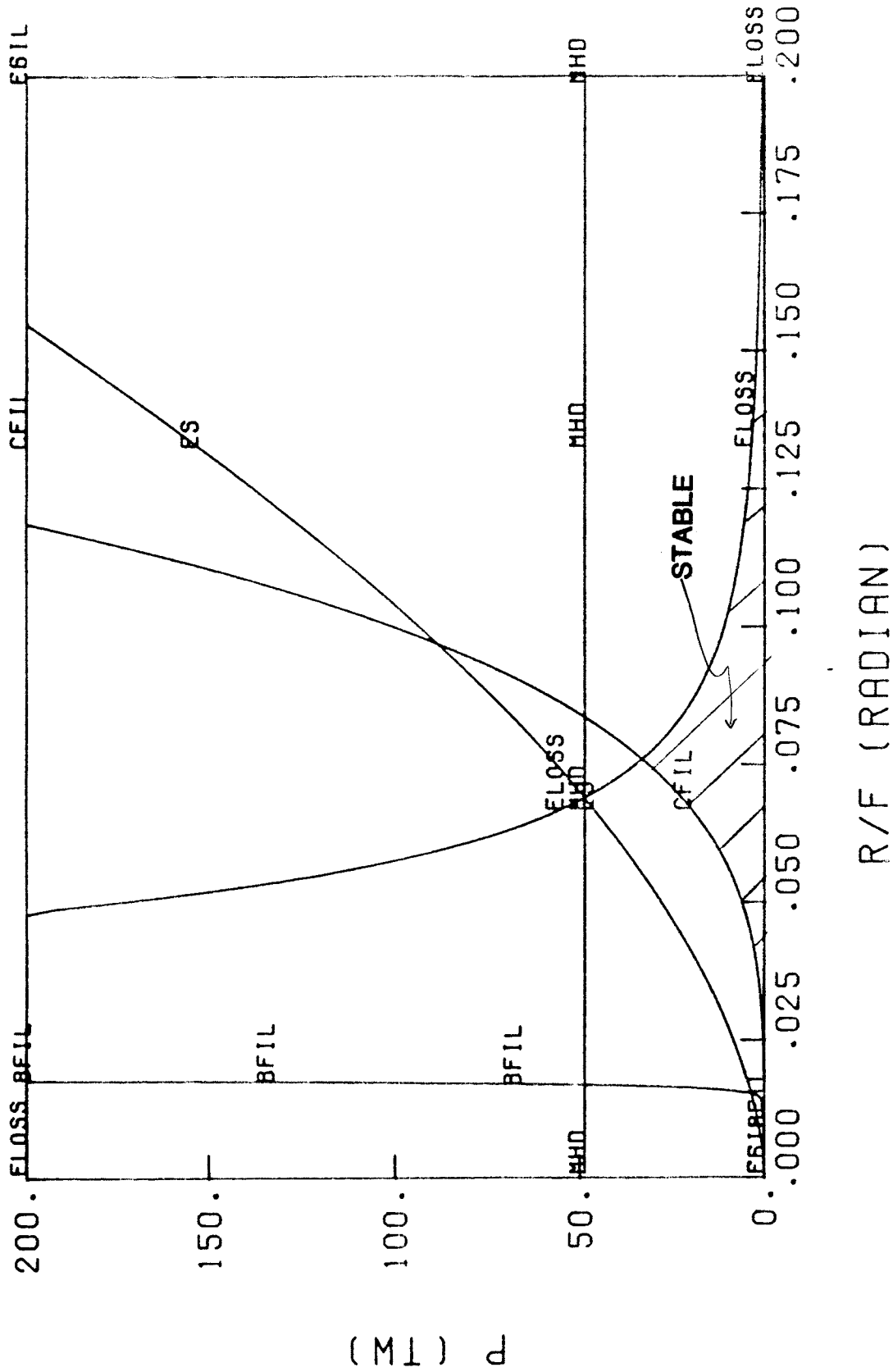
Fig. 3.8. Stability regions for a pulse of 30 MeV Li<sup>+3</sup> 17 ns long.



ABEAM=7.0 AMU ZBEAM=3.0 E RBEAM=.5 CM TBEAM=.5X10<sup>-7</sup> S X=1 EBAR=30 MEV

Fig. 3.9. Stability regions for a pulse of 30 MeV  $\text{Li}^{+3}$  50 ns long.





ABEAM= 7.0 AMU ZBEAM=3.0 E RBEAM= .5 CM TBEAM=.5000-07 S X=1.0 EBAR=64.0 MEV

Fig. 3.11. Stability regions for a pulse of 64 MeV  $\text{Li}^{+3}$  50 ns long.



One can see from these figures that the maximum allowable power per channel is very sensitive to the ion divergence and that this dependence is greatly affected by changes in the beam pulse width. This means that, if the beam is bunched in the channel, the allowable power per channel will change as the beam moves towards the target and that the channels must be carefully designed so that at no time does the power exceed the allowable value. The beam divergence, which is taken to remain constant throughout the beam propagation, should be optimized so that the highest upper limit on the power per channel is obtained. This optimization has been attempted in Table 3.2 where results are summarized for 15 MeV  $D^{+1}$ , 30 MeV  $Li^{+3}$  and 64 MeV  $Li^{+3}$  and for both bunched and unbunched scenarios. The big advantage of the unbunched option can be easily seen: since the beam pulse width does not change, the beam divergence can be chosen to give the maximum allowed power at the entrance to the channel, while in the bunched cases a compromise must be made. The 30 MeV  $Li^{+3}$  case looks to be in serious trouble even for the unbunched case, while the power per channel with bunching allowed by this stability analysis is one half what is called for by the design. Both the 15 MeV  $D^{+1}$  and the 64 MeV  $Li^{+3}$  options appear to be acceptable, though 64 MeV with bunching is only marginally so. Both the ION code and WINDOW code have been delivered to KfK and will be made operational on their computer system.

Analysis of ion propagation is continuing. We believe that we understand the state-of-the-art theory of ion propagation. This theory is at the stage where codes can be written to study specific beam characteristics and instabilities. We are pursuing the possible acquisition of such codes to serve as the basis for our continuing analysis.

### References for Section 3

1. P.F. Ottinger, D. Mosher and S.A. Goldstein, "Propagation of Intense Ion Beams in Straight and Tapered Z-Discharge Plasma Channels," *Phys. Fluids* 23, 909 (1980).
2. P.F. Ottinger, D. Mosher and S.A. Goldstein, "Microstability of a Focused Ion Beam Propagating Through a Z-Pinch Plasma," *Phys. Fluids* 22, 332 (1979).

3. P.F. Ottinger, D. Mosher and S.A. Goldstein, "Electromagnetic Instabilities in a Focused Ion Beam Propagating Through a Z-Discharge Plasma," Phys. Fluids 24, 164 (1981).
4. Ian Smith, private communication, May 1984.

#### 4. Mechanical Analysis of INPORT Units

The original analysis of INPORTs led to the development of a code to determine their dynamic response under repetitive impulsive loads. Variable parameters included length, diameter, damping, pretension and mass; the axial load gradient from gravity was replaced by its mean value. Late in 1983, the program was extended to include the effects of liquid metal flow velocity and parametric results were presented for repetition rates of 1.0 and 1.5 Hz.

Because INPORTs physically cover such unusually large spans, the effects of the axial tension gravity gradient have been a concern for accurate vibration analysis. An assessment of this has been recently completed for the planar problem. Normalized mode shapes and natural frequencies have been accurately calculated for the first ten modes. The results include the effects of variations in pretension loads and internal fluid velocity. Shifts occur in the position of peak modal amplitude and the magnitude of the natural frequencies, compared with the uniform tension case. For the LIBRA cavity it is important that factors influencing frequencies are identified, particularly for the lower mode, such that the design will avoid potential resonance problems from coincidence with repetition rate. Details of the analysis are represented in report FPA-84-2.

The second principal topic under development in 1984 is a study of the mechanical stability of the two-dimensional motion of INPORTs resulting from the sequential pressure pulses. It is known that simpler mechanical systems may initially oscillate in one plane but subsequently vibrate or whirl in an out-of-plane mode. The stability analysis is concerned with the circumstances under which this could occur for the LIBRA INPORTs. A very thorough development of the equations of motion has been completed; these are given in report FPA-84-3. The work includes viscous damping, gravity gradient, internal pressure, axial pretension and internal flow velocity. The equations can be used for tubes with flexural and/or extension stiffness. The most significant upgrade involves the development of the correct and consistent nonlinear terms for the equilibrium equations. Such terms are responsible for coupling between the two and three-dimensional modes.

The next phase of the work is computational, in which parametric response data will be obtained for the LIBRA cavity. The results will be important to determine if there is an interference or contact problem between INPORTs and

thus the considerations necessary for appropriate spacing in the design of the cavity.

## 5. Target Chamber Gas Dynamics

Two aspects of the flow of gas induced in the target chamber by the target microexplosion are currently under study: the propagation of the blast wave through the array of INPORT units and the vaporization of liquid metal off of the surface of the INPORT units. Both are at a stage where computational tools are being developed. Since January 1984, the previous work on blast waves over blunt bodies has been reviewed. Little work has been previously done on this subject for transient supersonic flow. The vaporization and condensation computer code CONRAD has undergone development and testing during this period.

The work on flow over the INPORT units reported for the last time period, December 1983, was from a macroscopic viewpoint in an effort to identify important characteristics of the tube response to the expanding blast wave. It was decided to begin a detailed modeling effort to resolve the blast wave interaction with the tube bank. This is important not only for the heat transfer characteristics, but the momentum transfer to the tubes will determine their mechanical response. Therefore, the work during this time period has focused on accumulating literature and computational tools to solve this problem.

The fluid flow over the tubes is essentially a transient high temperature blast wave problem characterized by low density and therefore low Reynolds number. Inquiries were made to the wind tunnel facilities at the U.S. Arnold Engineering and Development Center and Sandia National Laboratories for open test data in this field. Only global data exists for blast waves; no detailed flow structure or local pressure field data were located due to the extremely short time constant of interest. A literature review has revealed relatively few papers on the subject of numerical computation of blast waves and these were limited to modeling inviscid, isothermal flow (Euler's equation). The present problem requires the full Navier-Stokes equations, including an energy equation.

We have just acquired and installed a two-dimensional radiation hydrodynamics computer code with which we intend to perform detailed bounding calculations. Although this code solves the inviscid formulation of the fluid equations, it allows a pseudo-viscosity to be prescribed. It is felt that this code should provide reasonable overpressure loading for the first tube

bank and may determine if transient choking between the tubes will occur. We are also in the process of obtaining a full 3-D compressible flow Navier-Stokes code with energy transfer between the fluid and boundaries. After benchmark tests have been performed, this code should be capable of modeling the detailed flow between two tubes to determine if a wake-like flow will develop for the transient case.

After these efforts are underway, we also intend to evaluate the use of simulation methods for the Navier-Stokes equations (e.g., discrete vortex methods) for their applicability to the multibody problem. Detailed modeling of wake flows is still computationally intensive.

The condensation and vaporization computer code CONRAD has been undergoing development and testing. The code is derived from the multigroup radiative transfer hydrodynamics code, MF-FIRE.<sup>(1)</sup> Subroutines have been added which calculate the temperature profiles of a liquid metal layer by heat fluxes emanating from the gas. In LIBRA, the major component of these fluxes are the thermal photons from the fireball. Once the liquid metal reaches its local boiling temperature, vaporization is calculated thermodynamically. The vaporization of the liquid metal leads to a change of mass of the gas which has required the development of a dynamic rezoning of CONRAD's Lagrangian mesh. The models for condensation of the vapor back onto the walls is still under development.

The dynamic rezoning in CONRAD has been tested and energy has been found to be conserved during the process. The vaporization package has also been tested and has been found to agree with known cases.

#### References for Section 5

1. G.A. Moses, T.J. McCarville and R.R. Peterson, "MF-FIRE - A Multifrequency Radiative Transfer Hydrodynamics code," University of Wisconsin Fusion Engineering Program Report UWFDM-458, December 1982.